



# The NAD<sup>+</sup>-dependent protein deacetylase activity of SIRT1 is regulated by its oligomeric status

Xiumei Guo<sup>1</sup>, Mehmet Kesimer<sup>2\*</sup>, Gökhan Tolun<sup>3\*</sup>, Xunhai Zheng<sup>4\*</sup>, Qing Xu<sup>1</sup>, Jing Lu<sup>1</sup>, John K. Sheehan<sup>2</sup>, Jack D. Griffith<sup>3</sup> & Xiaoling Li<sup>1</sup>

<sup>1</sup>Laboratory of Signal Transduction, National Institute of Environmental Health Sciences, National Institutes of Health, Research Triangle Park, NC 27709, <sup>2</sup>Departments of Biochemistry and Biophysics, University of North Carolina at Chapel Hill, NC 27599, <sup>3</sup>Lineberger Comprehensive Cancer Center and Department of Microbiology and Immunology, University of North Carolina at Chapel Hill, NC 27599, <sup>4</sup>Laboratory of Structural Biology, National Institute of Environmental Health Sciences, National Institutes of Health, Research Triangle Park, NC 27709.

SIRT1, a NAD<sup>+</sup>-dependent protein deacetylase, is an important regulator in cellular stress response and energy metabolism. While the list of SIRT1 substrates is growing, how the activity of SIRT1 is regulated remains unclear. We have previously reported that SIRT1 is activated by phosphorylation at a conserved Thr522 residue in response to environmental stress. Here we demonstrate that phosphorylation of Thr522 activates SIRT1 through modulation of its oligomeric status. We provide evidence that nonphosphorylated SIRT1 protein is aggregation-prone *in vitro* and in cultured cells. Conversely, phosphorylated SIRT1 protein is largely in the monomeric state and more active. Our findings reveal a novel mechanism for environmental regulation of SIRT1 activity, which may have important implications in understanding the molecular mechanism of stress response, cell survival, and aging.

The sirtuins family of proteins are highly conserved NAD<sup>+</sup>-dependent protein deacetylases and/or ADP ribosyltransferases<sup>1</sup>. The seven mammalian sirtuins, collectively known as SIRT1 to SIRT7<sup>2</sup>, have emerged as crucial regulators for a variety of cellular processes, ranging from energy metabolism and stress response to tumorigenesis and possibly aging<sup>3</sup>. Previous studies have demonstrated that SIRT1, the most conserved mammalian sirtuin, directly couples NAD<sup>+</sup> hydrolysis to the deacetylation of numerous transcription factors and co-factors, including p53, E2F1, NFκB, FOXO, PGC-1α, c-myc, HIF-2α, HSF1, CLOCK and PER2, TORC2, as well as several nuclear receptors<sup>3</sup>. Therefore, SIRT1 directly links the cellular metabolic status to gene expression, playing an important role in a number of pro-survival and metabolic activities<sup>3,4</sup>.

While the list of SIRT1 targets is rapidly expanding, an intricate regulatory network that controls SIRT1 expression and activity has just begun to emerge<sup>5,6</sup>. This self-contained network functions at different levels and is critical for maintaining a suitable dosage of SIRT1 in response to various environmental stimuli. For example, SIRT1 transcription is under the control of multiple negative feedback loops that tightly regulate its activity in response to cellular stress<sup>7</sup>. SIRT1 expression is also regulated at the post-transcriptional level by both RNA binding proteins<sup>8</sup> and microRNAs<sup>9</sup>. Additionally, SIRT1 activity can be directly inhibited<sup>10,11</sup> or activated<sup>12,13</sup> by several protein factors, although the biology associated with these protein inhibitors and activators remains to be defined.

Studies from our laboratory and others have recently shown that the activity of SIRT1 can be modulated by phosphorylation modifications<sup>14–17</sup>. For instance, we have reported that SIRT1 can be phosphorylated and activated by two anti-apoptotic members of the DYRK family, DYRK1A and DYRK3<sup>17</sup>. These two kinases directly interact with SIRT1 and phosphorylate SIRT1 on threonine 522 (Thr522). This modification is sufficient to activate SIRT1, promoting cell survival in response to various environmental stresses. Interestingly, DYRK1A is an essential clock component that governs the rhythmic phosphorylation and degradation of CRY2 protein<sup>18</sup>. The DYRK1A-SIRT1 link revealed in our previous study suggests that DYRK1A may play a role in the circadian oscillation of SIRT1 activity<sup>19</sup>.

In this report, we show that phosphorylation of the Thr522 residue of SIRT1 activates its deacetylase activity through modulation of its oligomeric state. Non-phosphorylation of Thr522 leads to formation of less-active oligomers, whereas phosphorylation prevents formation of aggregates and results in SIRT1 activation. Therefore, our data unveil a novel mechanism that governs the environmental modulation of SIRT1 activity.

SUBJECT AREAS:  
MOLECULAR BIOLOGY  
POST-TRANSLATIONAL  
MODIFICATIONS  
BIOPHYSICS  
CELL SIGNALLING

Received  
11 May 2012

Accepted  
1 August 2012

Published  
7 September 2012

Correspondence and  
requests for materials  
should be addressed to  
X.L. (lix3@niehs.nih.  
gov)

\* These authors  
contribute equally to  
this study.

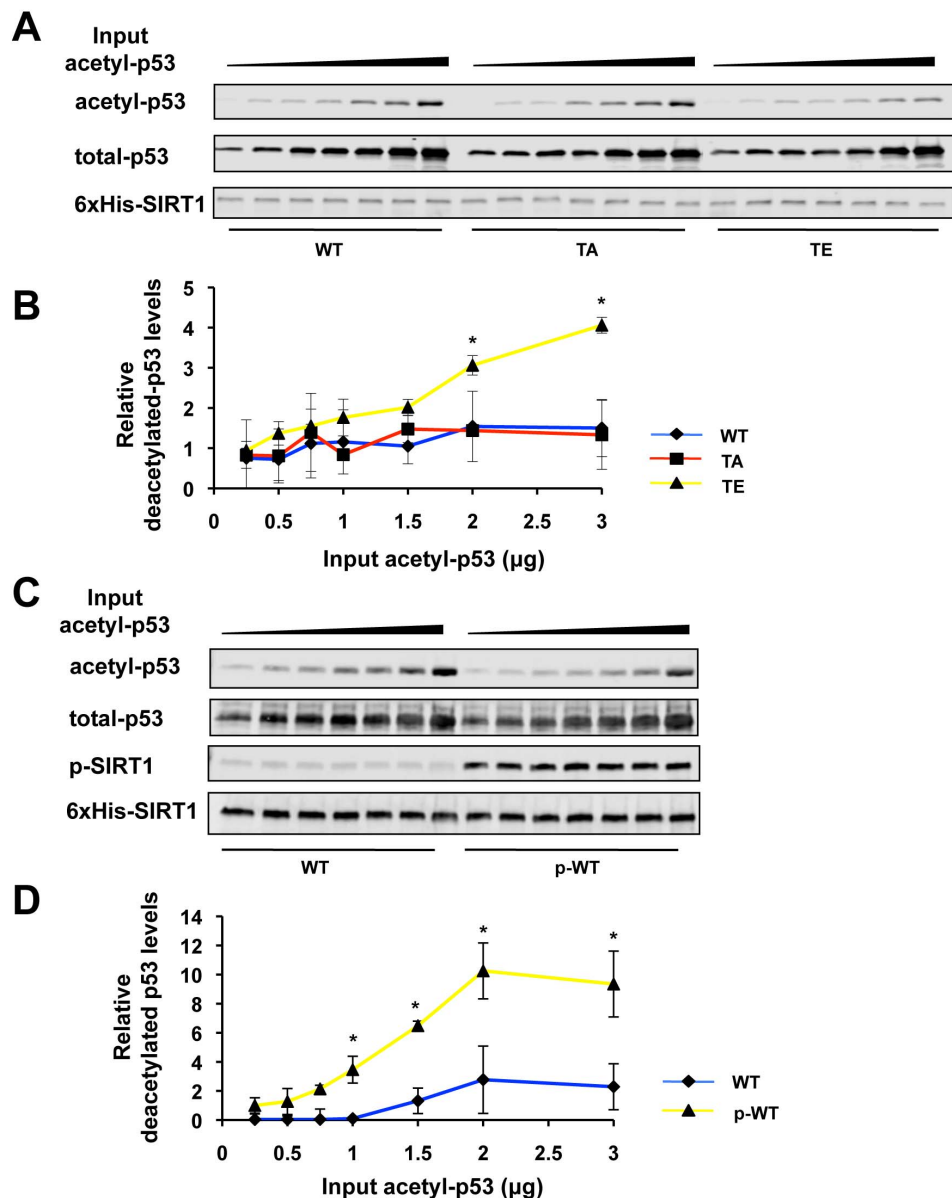


**Figure 1 | Phosphorylation of Thr522 activates SIRT1 *in vitro*.** (A) Representative *in vitro* enzymatic analysis of 6xHis tagged WT, TA, and TE SIRT1 proteins. 0.02 μg of purified recombinant WT, TA, or TE SIRT1 proteins were incubated with 0.25, 0.5, 0.75, 1.0, 1.5, 2.0, and 3.0 μg of *in vitro* acetylated GST-p53 fusion proteins in the presence of 3 mM of NAD<sup>+</sup> and 200 nM of TSA, and incubated at 37°C for 30 min. The acetylated GST-p53 levels were analyzed as described in the Methods. (B) Quantification of three independent *in vitro* enzymatic experiments in A. The total and acetylated GST-p53 levels were quantified as described in the Methods. (C) Representative *in vitro* enzymatic analysis of 6xHis tagged WT SIRT1 (WT) and DYRK1A-phosphorylated WT SIRT1 (p-WT) proteins. The assays were performed as described in (A) and the rate of deacetylated p53 levels were analyzed as described in the Methods. (D) Quantification of three independent *in vitro* enzymatic experiments as in C. The total and acetylated GST-p53 levels were quantified as described in the Methods. (\*,  $p < 0.05$ ).

## Results

**Phosphorylation of Thr522 activates SIRT1 on its native protein substrate.** To elucidate molecular mechanisms underlying the activation of SIRT1 by phosphorylation, we purified three recombinant 6xHis tagged proteins, wild-type SIRT1 (WT), a non-phosphorylation mimetic, SIRT1 T522A (TA), and a phosphorylation mimetic, SIRT1 T522E (TE), and analyzed their kinetic behaviors *in vitro* using acetyl-p53 as the substrate. Consistent with our previous observations with GST-tagged recombinant proteins<sup>17</sup>, all three SIRT1 proteins displayed comparable activities when acetyl-p53 levels were low (Figure 1A and 1B). However, the TE mutant was able to deacetylate p53 at a higher rate compared to the TA mutant when acetyl-p53 concentrations were increased. The recombinant WT SIRT1, which is nonphosphorylated at Thr522<sup>17</sup>, behaved similarly as the TA mutant

in this kinetic assay (Figure 1A). Further analyses of recombinant WT and DYRK1A-phosphorylated WT (p-WT) SIRT1 proteins confirmed that phosphorylation of Thr522 increased the activity of SIRT1, particularly at high substrate concentrations (Figure 1C and 1D). As the nonphosphorylated SIRT1 proteins (WT and TA) were still able to deacetylate low levels of acetyl-p53 at a comparable rate as the phosphorylated SIRT1 proteins (TE and p-WT), our data suggest that the intrinsic catalytic capacity of SIRT1 is not affected by the phosphorylation status of Thr522, yet the catalytic turnover of this enzyme is decreased when Thr522 is not phosphorylated.

**Non-phosphorylation of Thr522 leads to formation of SIRT1 protein aggregates *in vitro*.** The full-length murine SIRT1 protein consists of 737 amino acids that can be divided into an enzymatic



core domain and two flanking non-catalytic N- and C-terminal domains. The Thr522 residue is localized within a conserved hinge region linking the core domain and the C-terminal domain<sup>17</sup>. Although a recent study has shown that a 25 a.a. sequence located in the C-terminal domain is essential for SIRT1 activity<sup>20</sup>, previous structural studies have suggested that the N- and C-terminal extensions of sirtuins may function as inhibitory domains to regulate NAD<sup>+</sup> binding and protein substrate recognition<sup>21,22</sup>. Our observation that phosphorylation of Thr522 increases the activity of SIRT1 primarily at high substrate concentrations (Figure 1) suggests that introduction of a negatively charged phosphate group at this hinge region likely induces a conformational change that doesn't affect the intrinsic catalytic activity of SIRT1, but may help to reposition the inhibitory N and C-terminal domains, increasing the accessibility of protein substrates and/or release of protein products, thereby enhancing catalytic turnover and subsequent rounds of activity.

To confirm this hypothesis, we analyzed the conformations of the WT, TA, and TE SIRT1 proteins by various biophysical and biochemical methods. As shown in Figure 2A, dynamic light scattering analyses revealed that the TA and the TE mutants had distinct size distribution profiles in solution. The diameter of the TA mutant peaked around 25 nm, whereas the diameter of the TE mutant peaked around 18 nm, indicating that the phosphorylation mimetic is smaller than the non-phosphorylation mimetic. The diameter of the WT SIRT1, on the other hand, shifted from around 16 nm to 25 nm when the temperature increased from 4°C to 45°C (Figure 2A), suggesting that the nonphosphorylated recombinant WT SIRT1 protein is temperature sensitive. It behaves like the phosphorylated protein when temperature is low, but switches to the conformation of the nonphosphorylated protein when the temperature rises close to physiological or heat shock temperatures. Further sizing-column coupled multi-angle light scattering experiments performed at room temperature showed that the increased size of the TA mutant was due to aggregation of the mutant protein (Figure 2B). The TA mutant formed a heterogeneous mixture of oligomers which peaked around 300 to 400 kDa (Figure 2B, middle panel), whereas the TE mutant was eluted as a single smooth peak around 71 kDa which corresponds to the size of SIRT1 monomers (Figure 2B, bottom panel). Consistent with the dynamic light scattering data, the WT SIRT1 protein peaked around 211 kDa on the sizing column at room temperature, suggesting the existence of dimers/trimers (Figure 2B, top panel). Negative staining electron microscopy confirmed that the TA mutant formed heterogeneous aggregates, while the TE mutant was more uniform and smaller (Figure 2C and Supplementary Figure 1). Again, the WT SIRT1 protein appeared to form small oligomers (dimers or trimers) (Figure 2C and Supplementary Figure 1). Together, our data indicate that phosphorylation of Thr522 is essential to maintain the monomeric state of the SIRT1 protein. Keeping this site nonphosphorylated leads to oligomerization of SIRT1, and while removing the polar side-chain of Thr522 results in large protein aggregation.

**Phosphorylation of Thr522 decreases SIRT1 protein aggregates in cells and promotes cell survival in response to heat shock.** To confirm our *in vitro* biochemical observations that phosphorylation activates SIRT1 through prevention of protein oligomerization/aggregation, we transfected stable SIRT1 knockdown HEK293T cells (HEK293T T1RNAi) with constructs expressing an equal amount of untagged WT, TA or TE SIRT1 proteins (Supplementary Figure 2). The distribution of these proteins was then analyzed by Immuno-fluorescent staining and confocal microscopy imaging. As shown in Figure 3A and 3B, the WT SIRT1 protein, which can be phosphorylated by DYRKs or possibly other kinases in cells<sup>17</sup>, was evenly distributed in the nucleoplasm (top panels). The TE mutant displayed a similar pattern (bottom panels). The TA

mutant, on the other hand, was highly enriched near the periphery of nucleus (middle panels), suggesting that this non-phosphorylation mimetic is either prone to aggregation thus forming large clusters in cells, or cells are in the process of excluding this mutant from the center of nucleoplasm. We have previously shown that phosphorylation of Thr522 levels were significantly elevated after heat shock, a stress condition known to activate SIRT1<sup>23</sup>, and phosphorylation of Thr522 appears to be essential for SIRT1-mediated heat shock resistance<sup>17</sup>. To further confirm our above observations, we heat-shocked the HEK293T SIRT1 RNAi cells expressing WT, TA, and TE at 45°C for 15 min. The cells were then crosslinked with 0.1% glutaraldehyde on ice for indicated time, and the size distribution of these proteins was analyzed by SDS-PAGE and immunoblotting. As expected, increasing amounts of SIRT1 proteins migrated at higher molecular weight with increasing crosslinking time (Figure 3C). The WT SIRT1 protein and the TE mutant protein had a comparable amount of high molecular weight mass. The TA mutant protein, on the other hand, appeared to have more high-molecular weight aggregates, particularly after 30 min of crosslinking, indicating that this non-phosphorylation mimetic is prone to aggregation upon heat shock. Filter-dot blotting analyses of the crosslinked cell lysates displayed a similar pattern (Figure 3D). Taken together, these observations demonstrated that phosphorylation of Thr522 prevents the formation of SIRT1 aggregates in cultured cells.

To further investigate the role of Thr522 phosphorylation in cells, we generated two SIRT1 knockin mouse embryonic fibroblast lines (MEFs), SIRT1TAKI (TAKI) and SIRT1TEKI (TEKI) (Supplementary Figure 3). We first analyzed the stability of SIRT1 proteins in these cells upon heat shock treatment. As shown in Figure 4A, SIRT1 proteins from all three cells, wild-type (WT), TAKI, and TEK1, were relatively stable within 4 hours after heat shock treatment, indicating that heat shock treatment does not induce the degradation of SIRT1 proteins in cells. We then examine the formation of SIRT1 protein aggregates in these cells 30 min after heat shock treatment (Figure 4B). Although MEFs expressing the TA mutant protein did not appear to have increased high-molecular-weight SIRT1 aggregates after heat shock and crosslinking compared to the WT cells, the TE mutant cells displayed decreased amount of SIRT1 aggregates. This result supports our hypothesis that phosphorylation of Thr522 increases the conformational stability of SIRT1 protein in cells. We have previously shown that phosphorylation of Thr522 is required for the pro-survival activity of SIRT1 in cells in response to heat shock<sup>17</sup>. Consistent with this notion, the SIRT1 TE knockin MEFs had higher survival rate 24 hours after incubation at 45°C for 1 hour (Figure 4C). Collectively, these observations demonstrate that phosphorylation of Thr522 inhibits the formation of SIRT1 protein aggregates in cells, thereby activating SIRT1 and promoting cell survival in response to heat shock stress.

## Discussion

As the best-studied member of the sirtuins family, SIRT1 is rising as an important therapeutic target for a number of age-associated diseases and possibly aging. While much attention has been focused on the identification of cellular targets of this sirtuin, the network that regulates SIRT1 expression and activity has just begun to emerge<sup>3,5,6</sup>. We have recently shown that SIRT1 can be activated by phosphorylation at a highly conserved Thr522 residue in response to stress<sup>17</sup>. In the present study, we show that phosphorylation of this residue activates SIRT1 by preventing formation of less-active oligomers or aggregates *in vitro* (Figure 2) and in cells (Figure 3 and 4), which in turn promotes cell survival in response to heat shock in cultured cells (Figure 4). Our findings reveal a novel mechanism that governs the environmental modulation of SIRT1 activity, suggesting that small molecules that can modulate the oligomeric states of SIRT1 may improve cellular stress resistance in response to environmental stress (Figure 4D).



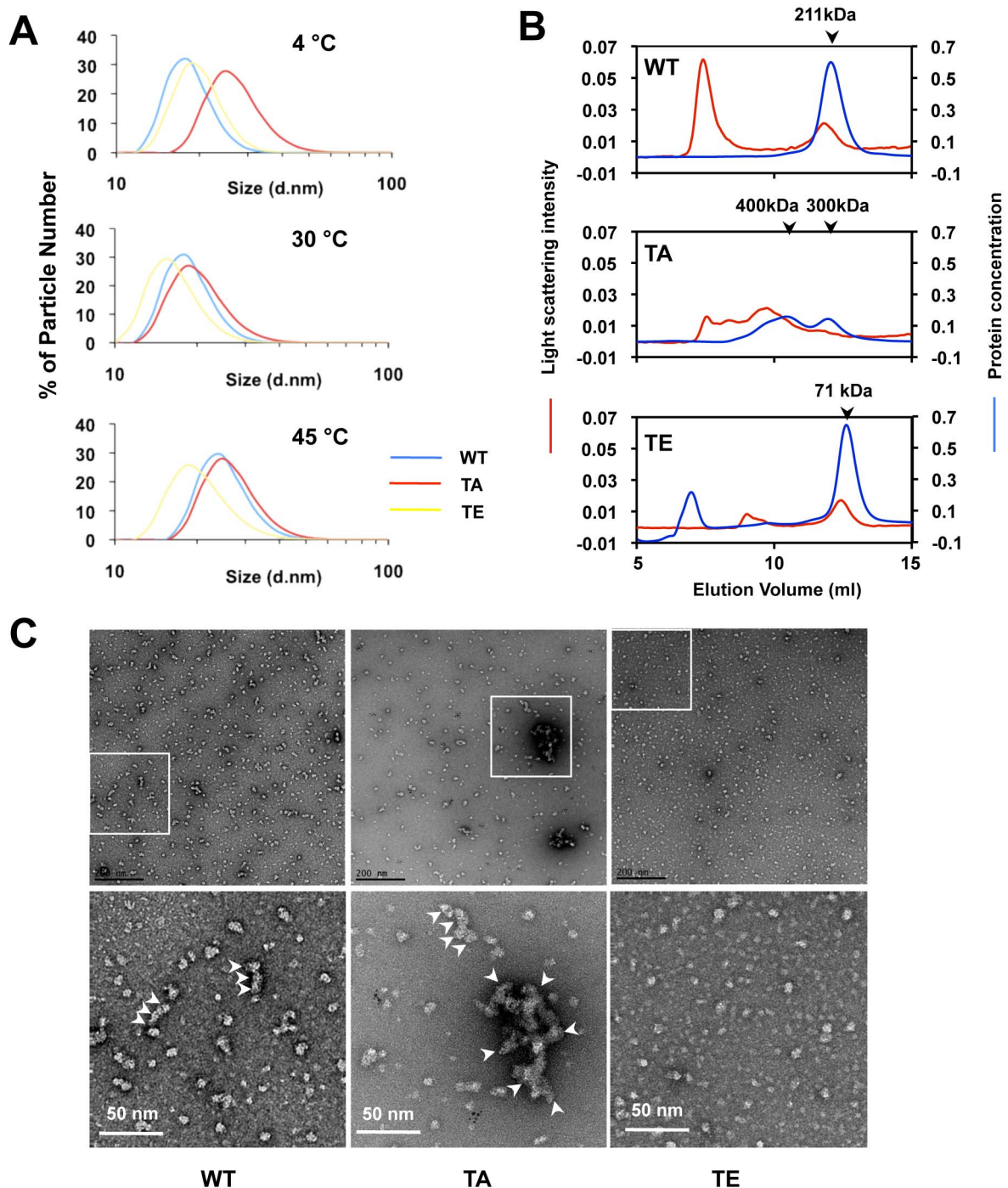


**Figure 2 | Non-phosphorylation of Thr522 results in formation of SIRT1 protein aggregates *in vitro*.** (A) The SIRT1 TE mutant proteins displays smaller size than nonphosphorylated SIRT1 proteins (WT and TA) in solution. Purified recombinant SIRT1 proteins were incubated overnight at 4, 30, and 45 °C respectively, and the solution size of these proteins were determined by dynamic light scattering as described in the Methods. (B) The nonphosphorylated SIRT1 proteins (WT and TA) are aggregation-prone, whereas the TE mutant proteins are primarily monomers in solution. Purified recombinant SIRT1 proteins were kept overnight at 4 °C and then analyzed at room temperature by sizing-column coupled multi-angle light scattering as described in the Methods and the molecular weight is calculated across the distribution. (C) Representative negatively stained EM images of samples used in B. Arrow heads mark SIRT1 oligomers and aggregates in the WT and TA samples.

Several lines of evidence suggest that although phosphorylation of Thr522 is essential for the pro-survival activity of SIRT1, the phosphorylation status of this residue does not affect the intrinsic catalytic activity of SIRT1, which is mechanistically different from a recently discovered phosphorylation modification located in the catalytic domain of SIRT1 (S434)<sup>24</sup>. For instance, phosphorylation of Thr522 does not affect the activity of SIRT1 *in vitro* when the protein

substrate concentrations are low (Figure 1), nor does it affect the deacetylase activity on small peptide substrates (not shown), which most likely reflects the intrinsic catalytic ability of SIRT1<sup>17,25</sup>. Instead, our data suggest that phosphorylation of Thr522 residue may promote the activity of SIRT1 through increasing its conformational stability in response to stress. Firstly, Thr522 phosphorylation does not affect the dynamic light scattering behavior of the nonphosphorylated

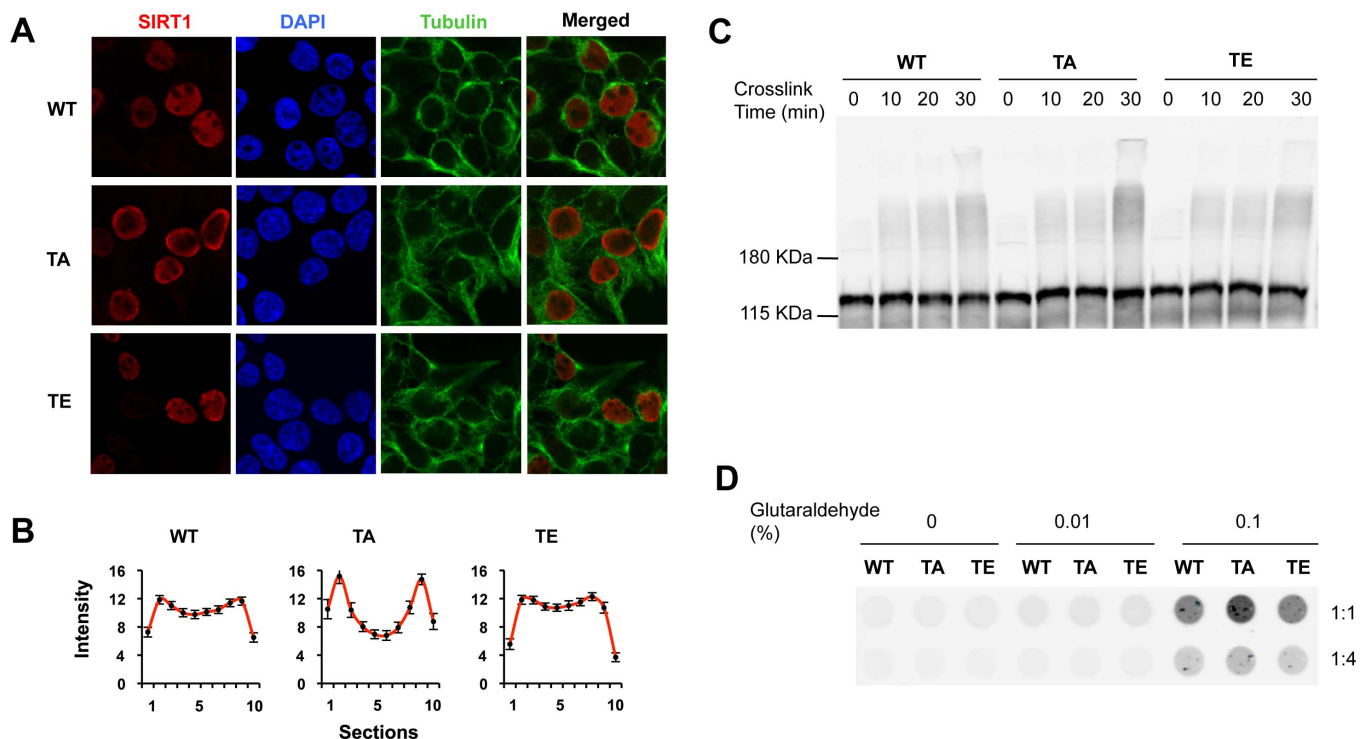


**Figure 3 | Phosphorylation of Thr522 activates SIRT1 through preventing the formation of less-active SIRT1 aggregates in cells.** (A) Abnormal accumulation of the SIRT1 TA mutant proteins near the peripheral of nucleus in cells. HEK293T T1RNAi cells were transfected with constructs expressing indicated SIRT1 proteins. The distribution of these proteins was analyzed by Immuno-fluorescent staining and confocal microscopy imaging as described in the Methods. (B) The distribution of SIRT1 WT, TA, and TE proteins in 100 nuclei from experiments in A was analyzed along the nuclear diameter as described in the Methods. (C–D) The SIRT1 TA mutant protein is prone to aggregation upon heat shock in cells. HEK293T T1RNAi cells transfected with constructs expressing indicated SIRT1 proteins were heat shocked at 45°C for 15 min and cooled down for 15 min on ice. Cells were then crosslinked with 0.1% glutaraldehyde/PBS on ice for indicated time (C) or 30 min (D) and analyzed by SDS-PAGE and immunoblotting (C) or filter dot-blotting (D) as described in the Methods.

recombinant WT SIRT1 proteins until the temperature rises close to physiological or stress temperatures (Figure 2A). Secondly, the non-phosphorylated SIRT1 proteins are prone to oligomerization in response to heat shock in cells (Figure 3 and 4). Thirdly, the Thr522 site is only highly conserved in mammals and birds<sup>17</sup>, two homeothermic animals with a body temperature significantly higher than the environmental temperature. Therefore, phosphorylation of Thr522 may be a conserved means for homeothermic animals to increase the thermal stability of SIRT1.

Mutation of threonine or serine to alanine has been routinely used to mimic the non-phospho-threonine or serine, while glutamate is well accepted as a phospho-threonine or serine mimetic. Our data indicate glutamate is an effective phospho-mimetic substitution for Thr522 of SIRT1 (Figure 1 and Figure 2). However, the alanine mutant (TA) is noticeably different from the WT recombinant SIRT1 that is nonphosphorylated at Thr522. For example, the WT SIRT1 protein only shows a similar solution size as the TA mutant at high temperature (Figure 2A), and forms small oligomers instead of large aggregates at room temperature (Figure 2B and 2C). These data suggest that the polar side-chain of Thr522 also plays a role in the maintenance of overall integrity of SIRT1 conformation and stability. Interestingly, when permanently knocked-in in MEF cells, the TA mutant does not appear to have any effect on SIRT1 oligomerization or activity (Figure 4B and 4C and Supplementary Figure 3C). One possible explanation is that phosphorylation of other residues in the nearby region induced by permanent dephosphorylation of Thr522 may compensate the effect of TA mutation. Further studies are needed to test this hypothesis. Nevertheless, our previous and present studies have demonstrated that phosphorylation of Thr522 is essential to activate SIRT1 in response to various environmental stresses,

and the TE mutant protein has effectively mimicked the effects of the Thr522 phosphorylation status both *in vitro* and in cells.

In summary, we have shown that phosphorylation of Thr522 is an important allosteric mechanism to activate SIRT1 in response to stress. While non-phosphorylation of this residue leads to formation of less-active oligomers, phosphorylation helps to maintain the monomeric status of SIRT1, resulting in increased activity. What remains to be determined is how phosphorylation status of Thr522 affects the diverse physiological functions of SIRT1 *in vivo*, and the precise role of this modification in various pathological conditions.

## Methods

**Plasmids and antibodies.** Untagged mouse SIRT1 was cloned in pcDNA3, or a modified 6xHis tag vector. The substitution mutants of SIRT1 were constructed by PCR-based site-directed mutagenesis. Anti-human SIRT1 and anti-mouse SIRT1 antibodies were from Sigma, anti-DYRK1A antibody was from Abnova and anti-DYRK3 antibody was from Santa Cruz Biotechnology. Anti-acetyl-p53 K382 antibody was from Abcam. Rabbit anti-p-Thr 522 antisera have been described<sup>17</sup>.

**Purification of recombinant SIRT1 proteins.** The plasmids encoding 6xHis-tagged SIRT1 proteins was transformed into BL21DE3 cells and the expression of 6xHis SIRT1 was induced with isopropyl-β-D-thiogalactopyranoside for overnight at 20°C. Cells were harvested and sonicated in 50 mM Tris-HCl, pH 8.0, 250 mM NaCl with 1 mM β-mercaptoethanol, 1x protease inhibitor (Roche cocktail). The supernatant was treated with Benzonase Nuclease (Sigma) for 30 min at room temperature to digest the nucleic acids. The 6xHis SIRT1 protein was then loaded nickel-nitrilotriacetic acid resin, washed with 50 mM Tris-HCl, pH 8.0, 250 mM NaCl, 1 mM β-mercaptoethanol, 20 mM imidazole, and eluted with 200 mM imidazole in 50 mM Tris-HCl, pH 8.0, 250 mM NaCl, and 1 mM β-mercaptoethanol. The SIRT1 fractions were pooled and further purified by gel filtration using superdex 200 columns using the same buffer.

**In vitro acetylation and deacetylation assays.** The *in vitro* acetylation of GST-p53 was carried out essentially as described<sup>26</sup>. To analyze the activity of SIRT1 *in vitro*,

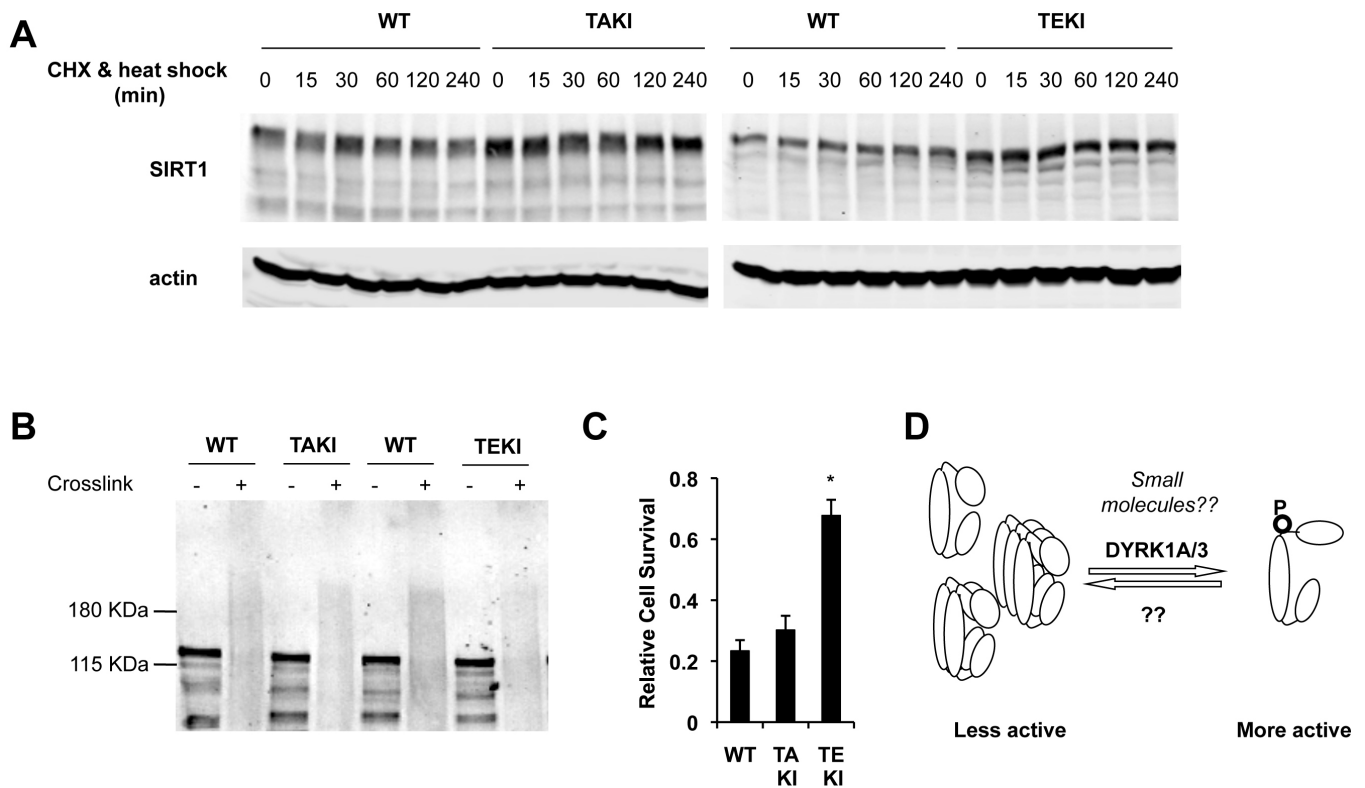


**Figure 4 | Phosphorylation of Thr522 prevents formation of SIRT1 aggregates and promotes cell survival in response to heat shock in knockin MEFs.** (A) The phosphorylation status of SIRT1 does not affect the degradation of SIRT1 proteins in MEFs upon heat shock treatment. The MEFs expressing endogenous WT SIRT1 proteins, or knocked-in TA (TAKI) or TE (TEKI) mutant proteins were incubated with 10  $\mu$ g/ml of cycloheximide (CHX) upon heat shock at 45°C, the levels of SIRT1 were analyzed by immuno-blotting at indicated time points after treatment. (B) The SIRT1 TE mutant proteins are protected from heat-shock induced aggregation in MEFs. Indicated MEFs were heat shocked at 45°C for 30 min and analyzed by crosslinking as described in the Methods. (C) The SIRT1 TE knock-in MEFs are more resistant to heat shock. Indicated MEFs were treated at 45°C for 1 h, and then recover at 37°C for 24 h. Cell viability was determined as described in the Methods. (D) Phosphorylation of Thr522 activates SIRT1 through preventing the formation of less-active SIRT1 oligomers. (\*,  $p < 0.05$ ).

purified wild-type SIRT1, SIRT1 mutants, and *in vitro* phosphorylated SIRT1 were kept at 4°C for overnight, then 0.02  $\mu$ g of indicated SIRT1 proteins were incubated with 0.25, 0.5, 0.75, 1.0, 1.5, 2.0, and 3.0  $\mu$ g of *in vitro* acetylated GST-p53 fusion proteins in the deacetylation assay buffer containing 50 mM Tris-HCl, pH 8.0, 137 mM NaCl, 2.7 mM KCl, 1 mM MgCl<sub>2</sub>, 1 mg/ml BSA, 3 mM of NAD<sup>+</sup> and 200 nM of TSA, and incubated at 37°C for 30 min. The total and acetylated GST-p53 levels were quantified with the Odyssey Infrared Imaging System (Li-Cor Biosciences) using anti-p53 and anti-acetyl-p53 K382 antibodies, and the relative deacetylated p53 levels were calculated against non-enzyme treated standards (not shown) and total p53 levels in each samples.

**Dynamic light scattering and multi-angle laser light scattering analyses.** To analyze the size of recombinant SIRT1 proteins in solution by dynamic light scattering assays, the protein samples (0.5 mg/ml) were analyzed using a Zetasizer Nano-S90 light scattering instrument (Malvern Instruments, Enigma Business Park, UK).

For multi-angle laser light scattering (MALLS) analysis, samples were chromatographed on a Superdex 200 HR (10/30 cm) size exclusion column and eluted with TBS buffer (0.2 M NaCl, 10 mM Tris, 10 mM EDTA, pH 7.0) at a flow rate of 0.3 ml/min. The column effluent was passed through an in-line enhanced optical system laser photometer (Dawn, Wyatt Technologies) coupled to a digital signal-processing interferometric refractometer (Optilab, Wyatt) to measure molecular weight and sample concentration, respectively. The Dawn MAALS measures the light scattered from the eluant at 18 angles between 10 and 150 degrees. The captured data were integrated and analyzed with the Astra software provided with the Dawn laser photometer.

**Negative staining and electronic microscopy imaging.** To analyze the ultrastructure of recombinant SIRT1 proteins, the samples were negatively stained with 2% uranyl acetate and examined in an FEI Tecnai 12 TEM (Hillsboro, OR). The images were recorded using a Gatan Inc. Ultrascan400 CCD camera (Pleasanton, CA). Obtained images were then analyzed by measuring the 2D projection areas of protein particles using ImageJ and Microsoft Excel, followed by statistical analysis by GraphPad Prism v5 (GraphPad Software, Inc., La Jolla, CA).

**Immuno-fluorescence assay.** Cells grown on coverslips were fixed with 4% paraformaldehyde in PBS at room temperature for 20 min. After washing three times

with PBS, cells were permeabilized with 0.2% Triton X-100 in PBS buffer for 10 min followed by additional washings. Coverslips were then incubated with primary antibodies (as indicated) in 10% FBS/PBS for 45 min at room temperature, followed by 10 min incubation with secondary antibodies. Finally, cells were counterstained with 4' 6-diamidino-2-phenylindole (DAPI) to visualize the nuclei. The slides were then analyzed on a Zeiss LSM 710 confocal microscope.

To quantify the distribution of SIRT1 proteins in the nucleus, the nuclear diameter from 100 random selected nuclei per sample were evenly divided into 10 sections. The intensity of SIRT1 immuno-fluorescent staining in each section was then quantified.

**Crosslinking.** To analyze the oligomeric status of WT, TA, and TE SIRT1 proteins in cells, HEK 293T SIRT1 RNAi cells transfected with indicated plasmids or WT, TA, and TE MEFs were cultured at 37°C or heat shocked at 45°C for 15 min or 30 min. The cells were then cooled down on ice for 15 min and crosslinked with 0.1% glutaraldehyde/PBS on ice for 30 min. Crosslinking was stopped by addition 100 mM glycine. Samples were then collected in SDS-PAGE sample buffer and boiled, and finally analyzed on 7.5% SDS-PAGE gel or filter-dot-blotting<sup>27</sup> followed by immuno-blotting with indicated antibodies.

**Cell viability assay.** MEFs were plated into 96-well plate at 50% confluence overnight. Cells were then treated at 45°C for 1 h, and then recover at 37°C for 24 h. Cell viability was determined with Cell Proliferation Reagent WST-1 (Roche Applied Science) according to the manufacturer's protocol.

**Statistical analysis.** Values are expressed as mean  $\pm$  standard error of mean (SEM). Significant differences between means was analyzed by two-tailed, unpaired Student's *t* test and differences were considered significant at  $p < 0.05$ .

- Blander, G. & Guarente, L. The Sir2 family of protein deacetylases. *Annu Rev Biochem* **73**, 417–35 (2004).
- Frye, R. A. Phylogenetic classification of prokaryotic and eukaryotic Sir2-like proteins. *Biochem Biophys Res Commun* **273**, 793–8 (2000).
- Haigis, M. C. & Sinclair, D. A. Mammalian sirtuins: biological insights and disease relevance. *Annu Rev Pathol* **5**, 253–95 (2010).





4. Schug, T. T. & Li, X. Sirtuin 1 in lipid metabolism and obesity. *Annals of Medicine* **43**, 198–211 (2011).
5. Kwon, H. S. & Ott, M. The ups and downs of SIRT1. *Trends Biochem Sci* **33**, 517–25 (2008).
6. Zschoernig, B. & Mahlknecht, U. SIRTUIN 1: regulating the regulator. *Biochem Biophys Res Commun* **376**, 251–5 (2008).
7. Brooks, C. L. & Gu, W. How does SIRT1 affect metabolism, senescence and cancer? *Nat Rev Cancer* **9**, 123–8 (2009).
8. Abdelmohsen, K. *et al.* Phosphorylation of HuR by Chk2 regulates SIRT1 expression. *Mol Cell* **25**, 543–57 (2007).
9. Yamakuchi, M., Ferlito, M. & Lowenstein, C. J. miR-34a repression of SIRT1 regulates apoptosis. *Proc Natl Acad Sci U S A* **105**, 13421–6 (2008).
10. Zhao, W. *et al.* Negative regulation of the deacetylase SIRT1 by DBC1. *Nature* **451**, 587–90 (2008).
11. Kim, J. E., Chen, J. & Lou, Z. DBC1 is a negative regulator of SIRT1. *Nature* **451**, 583–6 (2008).
12. Kim, E. J., Kho, J. H., Kang, M. R. & Um, S. J. Active regulator of SIRT1 cooperates with SIRT1 and facilitates suppression of p53 activity. *Mol Cell* **28**, 277–90 (2007).
13. Yang, Y. *et al.* SIRT1 sumoylation regulates its deacetylase activity and cellular response to genotoxic stress. *Nat Cell Biol* **9**, 1253–62 (2007).
14. Sasaki, T. *et al.* Phosphorylation regulates SIRT1 function. *PLoS One* **3**, e4020 (2008).
15. Kang, H., Jung, J. W., Kim, M. K. & Chung, J. H. CK2 is the regulator of SIRT1 substrate-binding affinity, deacetylase activity and cellular response to DNA-damage. *PLoS One* **4**, e6611 (2009).
16. Nasrin, N. *et al.* JNK1 phosphorylates SIRT1 and promotes its enzymatic activity. *PLoS One* **4**, e8414 (2009).
17. Guo, X., Williams, J. G., Schug, T. T. & Li, X. DYRK1A and DYRK3 promote cell survival through phosphorylation and activation of SIRT1. *J Biol Chem* **285**, 13223–32 (2010).
18. Kurabayashi, N., Hirota, T., Sakai, M., Sanada, K. & Fukada, Y. DYRK1A and glycogen synthase kinase 3beta, a dual-kinase mechanism directing proteasomal degradation of CRY2 for circadian timekeeping. *Mol Cell Biol* **30**, 1757–68 (2010).
19. Nakahata, Y. *et al.* The NAD<sup>+</sup>-dependent deacetylase SIRT1 modulates CLOCK-mediated chromatin remodeling and circadian control. *Cell* **134**, 329–40 (2008).
20. Kang, H. *et al.* Peptide switch is essential for Sirt1 deacetylase activity. *Mol Cell* **44**, 203–13 (2011).
21. Zhao, K., Chai, X., Clements, A. & Marmorstein, R. Structure and autoregulation of the yeast Hst2 homologue of Sir2. *Nat Struct Biol* **10**, 864–71 (2003).
22. Schwer, B., North, B. J., Frye, R. A., Ott, M. & Verdin, E. The human silent information regulator (Sir)2 homologue hSIRT3 is a mitochondrial nicotinamide adenine dinucleotide-dependent deacetylase. *J Cell Biol* **158**, 647–57 (2002).
23. Westerheide, S. D., Anckar, J., Stevens, S. M., Jr., Sistonen, L. & Morimoto, R. I. Stress-inducible regulation of heat shock factor 1 by the deacetylase SIRT1. *Science* **323**, 1063–6 (2009).
24. Gerhart-Hines, Z. *et al.* The cAMP/PKA pathway rapidly activates SIRT1 to promote fatty acid oxidation independently of changes in NAD(+). *Mol Cell* **44**, 851–63 (2011).
25. Blander, G. *et al.* SIRT1 shows no substrate specificity in vitro. *J Biol Chem* **280**, 9780–5 (2005).
26. Luo, J. *et al.* Negative control of p53 by Sir2alpha promotes cell survival under stress. *Cell* **107**, 137–48 (2001).
27. Scherzinger, E. *et al.* Huntingtin-encoded polyglutamine expansions form amyloid-like protein aggregates in vitro and in vivo. *Cell* **90**, 549–58 (1997).

## Acknowledgements

We thank Drs. Yanshun Liu, Paul Wade, and members of Li laboratory for critical reading and suggestions of the manuscript. We also thank Baozhong Zhao for technical supports, the NIEHS Protein Expression Core facility for large-scale protein purification, and the Fluorescence Microscopy and Imaging Center for helping in confocal imaging and data analyses. This research was supported by the Intramural Research Program of the NIH, National Institute of Environmental Health Sciences to X.L. (Z01 ES102205), and grants GM31819 and ES13773 to J.D.G.

## Author contributions

X. L. conceived the project, designed experiments, analyzed data, and wrote the manuscript. X. G. carried out experiments, analyzed data, and wrote the manuscript. M. K., G. T., X. Z., Q. X. and J. L. carried out experiments and analyzed data. J. K. S. analyzed data. J. D. G. designed experiments and analyzed data.

## Additional information

**Supplementary information** accompanies this paper at <http://www.nature.com/scientificreports>

**Competing financial interests:** The authors declare no competing financial interests.

**License:** This work is licensed under a Creative Commons Attribution-NonCommercial-NoDerivative Works 3.0 Unported License. To view a copy of this license, visit <http://creativecommons.org/licenses/by-nc-nd/3.0/>

**How to cite this article:** Guo, X. *et al.* The NAD<sup>+</sup>-dependent protein deacetylase activity of SIRT1 is regulated by its oligomeric status. *Sci. Rep.* **2**, 640; DOI:10.1038/srep00640 (2012).